Electronic Supplementary Information (ESI)

Temperature-driven self-actuated microchamber sealing system for highly integrated microfluidic devices

Toyohiro Naito,*[a] Rerngchai Arayanarakool,[b] Séverine Le Gac,[b] Takao Yasui,[a] Noritada Kaji,[a] Manabu Tokeshi,[c] Albert van den Berg[b] and Yoshinobu Baba[a,d]

[a] *Department of Applied Chemistry, Graduate School of Engineering, Nagoya University, Furo-cho, Chikusa-ku, Nagoya 464-8603, Japan. FIRST Research Center for Innovative Nanobiodevices, Nagoya University, Furo-cho, Chikusa-ku, Nagoya 464-8603, Japan. Fax: +81 52 7894666; Tel: +81 52 7893560; E-mail: naito.toyohiro@f.mbox..nagoya-u.ac.jp*

[b] *BIOS. The Lab-on-a-Chip Group, MESA+ Institute for Nanotechnology, University of Twente, Postbus 217, 7500 AE Enschede, The Netherlands.*

[c] *Division of Biotechnology and Macromolecular Chemistry, Faculty of Engineering, Hokkaido University, Kita 13 Nishi 8, Kita-ku, Sapporo 060-8628, Japan.*

[d] *Health Research Institute National Institute of Advanced Industrial Science and Technology (AIST), Hayashi-cho 2217-14, Takamatsu 761-0395, Japan.*

** Corresponding author.*

Comparison of the optical properties

Refracrive indexes and Transmittances of cured NOA81, glass, quartz, poly(dimethylsiloxane) (PDMS), poly(methyl methacrylate) (PMMA), polycarbonate (PC), polystyrene (PS) and cyclic olefin copolymer (COC) were made a table. (Table S1) Data for NOA81, PDMS, PMMA, PS, PC and COC are from mnufactures' data sheets, and data for glass and quartz are from a handbook of chemistry and physics published by CRC press.

Table S1 Comparison of the optical properties

	NOA81	Glass	Quartz	PDMS	PMMA	PS	PC	COC
Refractive index	1.56	1.46	1.544	1.4118	1.491	1.59	1.586	1.53
Transmittance@589 nm	91	93	92	94	92	91	88	92

Fabrication scheme of the NOA 81-based multilayer device

SU-8 based masters were fabricated using photolithography techniques on a silicon wafer (Fig. S1 (1)). As indicated at the top of Figure S1, the negative photoresist SU-8 50 (Microchem., MA) formed a 50 μm resist layer on all layers with masks. These SU-8-based moulds were used for the realization of PDMS moulds (Figure S1 (2)). The resulting chips were subsequently cleaned in ethanol in an ultrasonic bath for 15 min and carefully dried using compressed air before being used for the channel fabrication (Fig. 2 (3) i-v).

Three sets of interspaces were made, consisting of NOA sheets for a lid layer and a reaction chamber layer (i and ii in Fig. S1 (4)), a membrane layer and a main channel layer (iii and iv) and a pneumatic chamber layer (Si substrate and v). A UV-curable adhesive, NOA 81 precursor was injected and allowed to spread slowly into the interspaces by capillary action prior to a 90 s curing step by UV irradiation (Fig. S1 (5),(6)). PDMS moulds for the pneumatic chamber and membrane were peeled from the formed NOA 81 sheets and two NOA 81 sheets were bonded by UV irradiation for 30 s (right image in Fig. S1 (7)). Two access holes for sample introduction were punched in the NOA 81 sheet used for the lid after peeling off the two PDMS moulds for the lid (left image in Fig. S1 (7)). Finally, the PDMS mould for the main channel on the NOA sheets bonded to the Si substrate was the peeled off the laminated NOA sheets, and the assembled NOA sheets were bonded by UV irradiation for 3 min (Fig. S1 (8)).

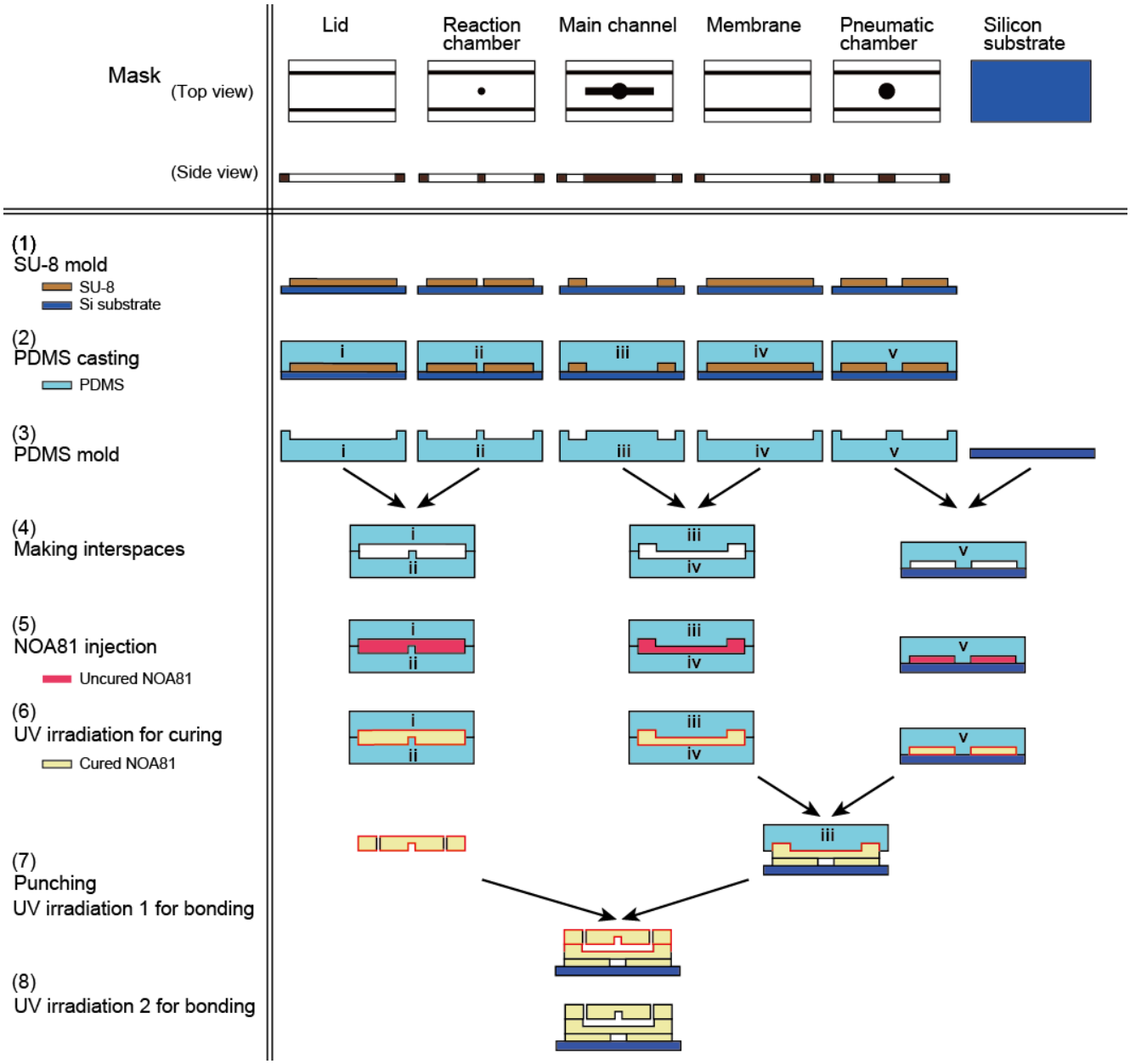

Fig. S1 Fabrication scheme of a NOA 81-based multilayer device

Definition of channel area

The differential edge detection method which is a combination of the first and second derivative of a fluorescence intensity profile was used to define the channel area. Fluorescence intensity is dramatically increased around the channel sidewalls (Fig. S2, (b)), and the change causes a peak and a trough in the first derivation (Fig. S2, (c)) and two sets of a peak and trough in the second derivation (Fig. S2, (d)). The zero value between the peak and the trough in the second derivation profile was defined as at the channel sidewalls.

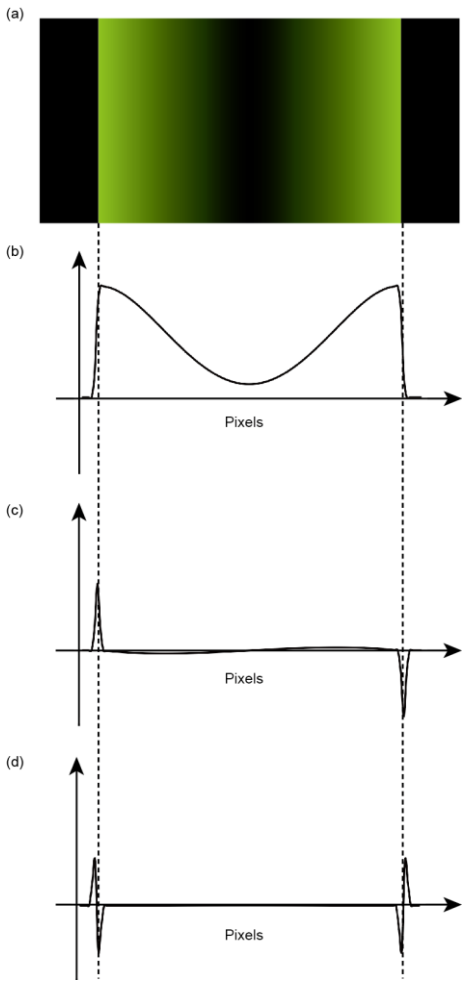

Fig. S2 (a) Illustration of a fluorescence image of a channel. (b) Intensity profile of the illustration in (a). (c) The corresponding first derivative profile. (d) The corresponding second derivative profile.

Derivation of the equation of the elastic curve

The membrane deflection is illustrated in Fig. S3. The membrane is considered as the continuum of beams that have both ends fixed; that is, bars with undeformable ends. The beam bending curve under a uniformly distributed load can be expressed as eqn (S1).

$$EI\frac{d^4\delta(x)}{dx^4} = w \qquad \text{(S1)}$$

E is Young's modulus, *I* is the second moment of area (*EI* is known as flexural rigidity), *x* is distance from *A*, $\delta(x)$ is z-axial displacement of the beam deformation at position *x* and *w* is load on the beam. From eqn (S1), we obtain the following by integrating in *x* (C_1–C_4 are integral constants).

$$EI\frac{d^3\delta(x)}{dx^3} = wx + C_1 \qquad \text{(S2)}$$

$$EI\frac{d^2\delta(x)}{dx^2} = \frac{1}{2}wx^2 + C_1x + C_2 \quad \text{(S3)}$$

$$EI\frac{d\delta(x)}{dx} = \frac{1}{6}wx^3 + \frac{1}{2}C_1x^2 + C_2x + C_3 \quad \text{(S4)}$$

$$EI\delta(x) = \frac{1}{24}wx^4 + \frac{1}{6}C_1x^3 + \frac{1}{2}C_2x^2 + C_3x + C_4 \quad \text{(S5)}$$

When a load is on the beam, eqns (S2) to (S5) satisfy the boundary conditions given in eqns (S6) to (S9) because the ends cannot deform, nor can they tilt up.

$$\delta(0) = 0 \quad \text{(S6)}$$

$$\delta(l) = 0 \quad \text{(S7)}$$

$$\frac{d\delta(0)}{dx} = 0 \quad \text{(S8)}$$

$$\frac{d\delta(l)}{dx} = 0 \quad \text{(S9)}$$

Here l is the beam length, x = l at B. Substituting these values into eqns (S4) and (S5) and solving for C_1–C_4 we have

$$C_1 = -\frac{1}{2}wl$$

$$C_2 = \frac{1}{12}wl^2$$

$$C_3 = 0$$

$$C_4 = 0$$

which we substitute into eqn (S5).

$$\delta(x) = \frac{w}{24EI}x^4 - \frac{wl}{12EI}x^3 + \frac{wl^2}{24EI}x^2 \quad \text{(1)}$$

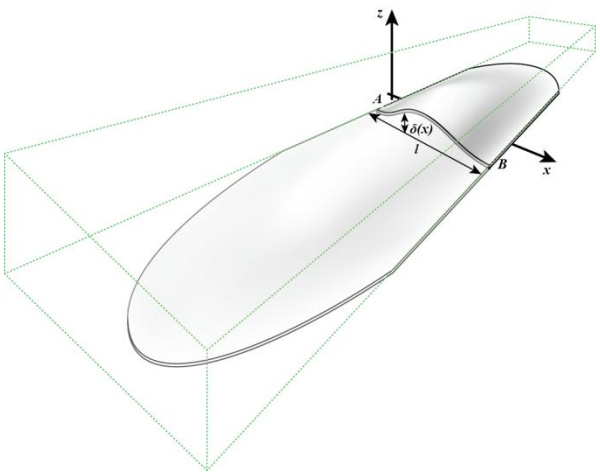

Fig. S3 Condition for membrane deformation in the channel

Independence of membrane deflection on volume of a pneumatic chamber

To prepare three pneumatic chambers with different volumes, the depth of the pneumatic chamber was changed for a fixed base area. Figure S2 shows at 60ºC the membrane deflection has no relationship to the depth of the pneumatic chamber; this temperature gives the highest R^2 value among all three depths. The relationship is consistent with the gas law; pressure is constant if molecular volume of gases is kept constant at the same temperature.

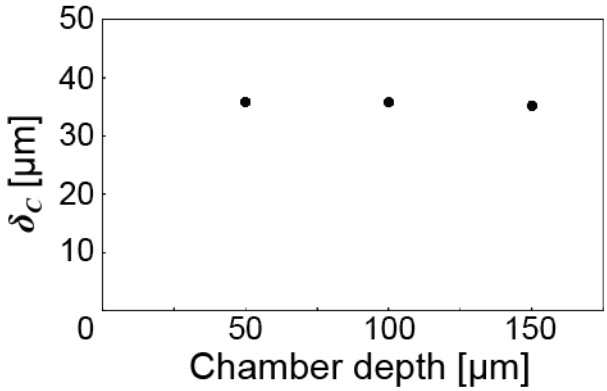

Fig. S4 Relationship between the membrane deflection and the depth of the pneumatic chamber

Valve opening and closing operations during thermal cycling

The device we fabricated was a repeatable valve as seen in the movie Movie S1. The valve repeated closing and opening operations during five repeated temperature cycles (95ºC for 30 s, 75ºC for 30 s, 55ºC for 30 s). Movie S1 plays at 64× the actual speed.